Surface-emitting second-harmonic generation in a semiconductor vertical resonator

R. Lodenkamper, M. L. Bortz, M. M. Fejer, K. Bacher, and J. S. Harris, Jr.

Stanford University, Stanford, California 94305

Received July 6, 1993

We experimentally demonstrate a 240-fold increase in the efficiency of an AlGaAs/AlAs surface-emitting second-harmonic generation device by embedding the waveguide core in a monolithic vertical resonant cavity. Calculations indicate that conversion efficiencies of several percent per watt for second-harmonic generation of green or blue light may be expected in an optimized semiconductor resonant vertical-cavity surface emitter.

Surface-emitting second-harmonic generation (SHG) has been demonstrated as a means for generating visible radiation in monolithic waveguide structures.[1,2] These devices, with interaction lengths of a waveguide core thickness, are inefficient when compared with collinearly phase-matched SHG devices, which can have much longer interaction lengths. Thus surface emitters are advantageous primarily when a competing collinear device is unavailable; for example, if the medium is not collinearly phase matchable, is lossy at the second harmonic, or must be monolithically integrated with the pump laser. However, surface emitters have efficiencies that are too low to permit them to serve as practical sources of coherent radiation. One way to increase efficiency is to resonate the fundamental and/or the second-harmonic field, as has long been known for collinear devices.[3] In this Letter we describe an experimental demonstration of the effect of resonance of the second harmonic in a monolithic AlGaAs vertical-cavity surface-emitting structure.

In a surface emitter two counterpropagating pump modes in a waveguide generate a nonlinear polarization that is a slowly varying function of z, the waveguide propagation direction. The component of the nonlinear polarization that oscillates in the plane of the waveguide can then radiate in a near-surface-normal direction. Figure 1 shows a side view of a vertically resonant surface emitter. For simplicity, we assume a TE pump, a homogeneous cavity, and no nonlinearity in the mirrors. In the nondepleted-pump approximation, the on-resonance conversion efficiency[4] of a doubly resonant vertical-cavity surface emitter with a TE slab waveguide mode pump is given by

$$\frac{P_o}{P_i^2} = C\,\frac{L}{w}\left[\frac{16T_{2\omega}}{(T_{2\omega}+\delta_{2\omega})^2}\right]\left[\frac{4T_{\omega}}{(T_{\omega}+\delta_{\omega})^2}\right]^2. \qquad (1)$$

Here $C = 32\pi^2J^2/N_e^{\,2}n_{2\omega}\epsilon_0 c\lambda_0^{\,2}$ (with N_e the effective index of the fundamental waveguide mode, $n_{2\omega}$ the index of the cavity at the second harmonic frequency, and λ_0 the free-space wavelength of the fundamental), L is the length of the device, w is the width of the fundamental mode, T_{ω} and $T_{2\omega}$ are the power transmissions of the coupling mirrors at the fundamental and second harmonic, respectively, and similarly δ_{ω} and $\delta_{2\omega}$ are the total cavity power losses (assumed small), excluding the coupling mirror transmissions. For a device with a nonresonant fundamental, the last factor in Eq. (1) can be set equal to one if the backward-propagating pump wave is provided by an ideal ($R = 1$) endface reflection. The overlap integral J is given by

$$J = \int_{-\rho}^{\rho} d_{\mathrm{eff}}(x)E_y^{\,2}(x)\cos(k_{2\omega}x)\mathrm{d}x\,, \qquad (2)$$

where E_y, the modal electric field of the fundamental, is normalized so that $\int_{-\infty}^{\infty}E_y^{\,2}\mathrm{d}x = 1$, d_{eff} is the effective nonlinear coefficient, 2ρ is the thickness of the waveguide core, and $k_{2\omega}$ is the wave number of the second harmonic in the cavity medium.

To facilitate subsequent numerical estimates, we evaluate J for the lowest-order TE mode of a symmetric slab waveguide with $E_y(x)$ given by

$$E_y(x) = \begin{cases} A\cos(Ux/\rho) & |x| \le \rho \\ A\cos(U)\exp[W(1-|x/\rho|)] & |x| \ge \rho \end{cases}, \qquad (3)$$

where $A = [W/\rho(W+1)]^{1/2}$, $U = 2\pi\rho(n_{\mathrm{co}}^{\,2} - N_e^{\,2})^{1/2}/\lambda_0$, and $W = 2\pi\rho(N_e^{\,2} - n_{\mathrm{cl}}^{\,2})^{1/2}/\lambda_0$. The index of the core is n_{co}, the index of the cladding is n_{cl}, and the modal effective index N_e is determined by the eigenvalue equation $W = U\tan(U)$. For simplicity, we assume the mirror phase shifts are such that the cavity resonance condition for the

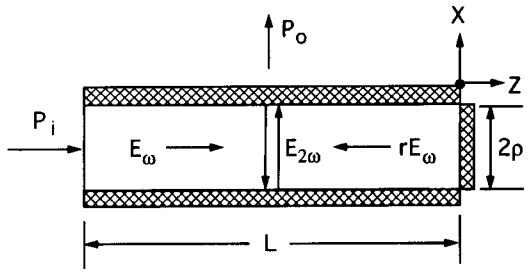

Fig. 1. Schematic side view of a vertically resonant surface-emitting SHG device. The hatched areas are mirrors, and the backward-propagating pump wave, rE_{ω}, is provided by an endface reflection. A circulating second harmonic, $E_{2\omega}$, is built up inside the cavity.

0146-9592/93/211798-03$6.00/0

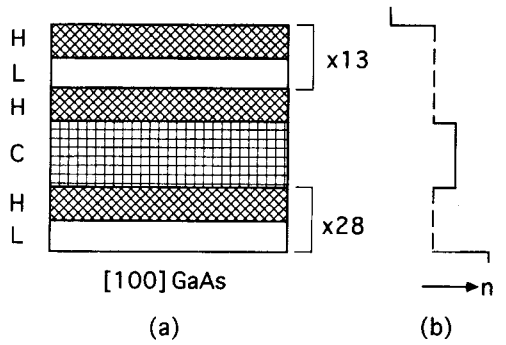

Fig. 2. (a) Epitaxial layer design for our sample. The quarter-wave layers, labeled H and L, have Al mole fractions of 0.5 and 1.0, respectively. The layer labeled C is the core/cavity layer, with an Al mole fraction of 0.6 and a thickness of 0.68 μm (seven half-waves of the harmonic). (b) Schematic index profile of the structure at 1.32 μm, where the dashed lines represent the form-birefringent indices (which are approximately equal on this scale) of the mirrors at 1.32 μm.

second harmonic is $2k_{2\omega}\rho = m\pi$, where m is an integer. Evaluating Eq. (2) for the mode given by Eq. (3), we find

$$|J| = \frac{d_{\text{eff}}}{\rho}\frac{W}{W+1}\frac{2}{k_{2\omega}}\left|\frac{1}{2} - \frac{m^2\pi^2\cos(2U)}{32U^2 - 2m^2\pi^2}\right| \quad m \text{ odd}, \tag{4}$$

for the magnitude of J. For even m, J is significantly smaller, so m should be odd to maximize efficiency. From Eq. (4) we see that the overlap integral scales as the product of four factors: $1/\rho$, an effective confinement factor, a coherence length, and an interference factor of the order of unity. The efficiency can be significantly increased by quasi-phase matching,[5] e.g., by changing the sign or magnitude of d_{eff} periodically in order to reduce destructive interference in Eq. (2). In that case, we see from Eq. (2) that J should be of the order of d_{eff} for a well-confined fundamental mode and ideal quasi-phase matching, in which the sign of d_{eff} changes every half-wavelength of the harmonic.

We chose AlGaAs as a convenient material system for a proof-of-principle device and used a fundamental wavelength of 1.32 μm since AlGaAs is not sufficiently transparent at wavelengths shorter than 660 nm to demonstrate significant resonant enhancement. Figure 2 shows the design of the epitaxial layers. The structure incorporates a single-mode planar waveguide at 1.32 μm inside a vertical cavity that is resonant at 660 nm. The nominal reflectivities of the top and bottom mirrors are 95% and 99.5%, respectively, so the theoretical resonant enhancement, calculated from Eq. (1) assuming no material loss, is a factor of 264.

The structure was grown by molecular-beam epitaxy. *In situ* reflectivity measurements[6] were used to correct the growth rates so that the quarter-wave mirrors were centered at 660 nm and the cavity mode resonance at the center of the wafer was at a slightly longer wavelength than 660 nm. The radial wafer nonuniformity ensured that a 660-nm resonance region would exist in a ring at some distance from the center of the wafer, as shown in the inset of Fig. 3. This wafer nonuniformity was used to measure the resonance effect. The second-harmonic output from a slightly nonuniform device will have a Lorentzian dependence on position, with a FWHM given by

$$\text{FWHM} = \left(\frac{d\lambda_c}{dz}\right)^{-1}\left[\frac{\lambda_c}{2\pi m}(T_{2\omega} + \delta_{2\omega})\left(\frac{\Delta n}{\Delta n + n_c/m}\right)\right], \tag{5}$$

where the factor in square brackets is the wavelength FWHM[7] of the cavity, Δn is the index difference between the high- and low-index mirror layers, λ_c is the free-space resonant wavelength of the cavity, n_c is the index of the cavity layer at λ_c, and $d\lambda_c/dz$ is the slope of the resonant wavelength as a function of radial position, a measure of the wafer nonuniformity. For our device, $\Delta n = 0.37$, $m = 7$, and $n_c = 3.40$, and Fig. 3 shows data, taken with a white-light source and a spectrometer, that give $d\lambda_c/dz = 0.62$ nm/mm at $\lambda_c = 659.5$ nm.

Since the dominant surface-emitting nonlinear polarization term in our device is $P_y = 4\epsilon_0 d_{14}E_xE_y$, where the x and y subscripts refer to the coordinates given in Fig. 1, we must launch both a TE mode and a TM mode in order to obtain SHG. The modal birefringence of the waveguide will then cause the near-field SHG output power to have a z dependence of the form $\cos^2(\Delta\beta z)$, where $\Delta\beta = \beta_{\text{TE}} - \beta_{\text{TM}}$ is the modal birefringence of the fundamental. Thus the expected functional form of the second-harmonic output is given by

$$P_o(z) = A_1\cos^2(A_2z + A_3)\{1 + [(z - A_4)/A_5]^2\}^{-1}, \tag{6}$$

the product of a periodic mode beating and a Lorentzian envelope.

The device was operated as a single-mode planar waveguide. The required lateral confinement

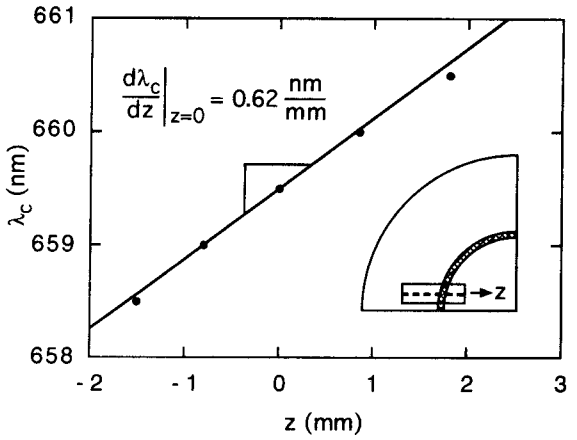

Fig. 3. Cavity resonance wavelength versus position. The filled circles are data points, and the solid line is a linear approximation to the data at $z = 0$. The inset shows the relationship of the cleaved sample (the rectangle) to the on-resonance region of the molecular-beam epitaxy wafer (the hatched region). The second-harmonic output from the sample is indicated by the dashed line.

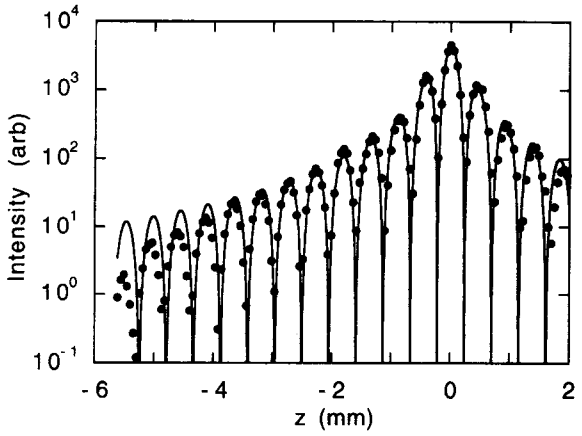

Fig. 4. Second-harmonic intensity versus position. The filled circles are data points, and the solid curve is a fit according to Eq. (6).

was provided by anamorphic input coupling optics, namely, a 63× microscope objective and a 127-mm focal-length cylindrical lens, which were used to end fire a 150-mW beam of 1.32-μm Nd:YAG laser radiation approximately 50 μm wide into the waveguide. The input beam was polarized at 45 deg to the plane of the waveguide in order to launch both TE and TM modes. The backward-propagating modes were generated by reflection from the cleaved endface.

The inset of Fig. 3 shows the relation of the second-harmonic output to the nonuniformity of the sample. The top surface of the sample was imaged onto a 0.1-mm slit, which was moved in 0.1-mm increments in tandem with a photomultiplier tube to take the line scan shown in Fig. 4. The periodic oscillations in the 660-nm output are due to the TE–TM mode beating. The variation of the envelope of the oscillations shows a strong vertical resonance effect, with a contrast ratio of at least 500:1. Since the square root of the contrast ratio gives only a lower bound of the resonant enhancement, we characterized the resonance effect by making additional measurements to determine the cavity parameters $T_{2\omega}$ and $\delta_{2\omega}$ and then used Eq. (1) to estimate the resonant enhancement. The solid curve in Fig. 4 is a fit to a function of the form given in Eq. (6). The relevant curve-fitting parameter is the FWHM of the Lorentzian envelope, which is 0.55 mm. With this value in Eq. (5) we obtain a total cavity loss of $T_{2\omega} + \delta_{2\omega} = 0.052$.

To estimate the output coupling and the cavity loss independently, we measured the reflectivity of our sample as a function of position for a beam of 660-nm light. The light source was a 1.32-μm Nd:YAG-laser-pumped $LiNbO_3$ waveguide frequency doubler,[8] whose 660-nm output was focused to a 60-μm-diameter spot on the sample. The measured minimum reflectivity was 0.26. By combining previous results with the following relation for the minimum reflectivity of a low-loss Fabry–Perot interferometer: $R_{\min} = (T_{2\omega} - \delta_{2\omega})^2/(T_{2\omega} + \delta_{2\omega})^2$, and assuming that $T_{2\omega} > \delta_{2\omega}$, we find $T_{2\omega} = 0.039$ and $\delta_{2\omega} = 0.013$. By substituting these cavity parameters into Eq. (1), we find a resonant enhancement of approximately 240 for this sample, which is quite close to the nominal value of 264.

For application of this technique to shorter wavelengths, films with lower visible absorptivity than AlAs/AlGaAs are necessary. Consider, for example, a monolithic vertical-cavity ZnSe/ZnS device that doubles 1064-nm light to 532 nm. We assume that $n_{co} = 2.47$, $n_{2\omega} = 2.68$, and $d_{eff} = 80$ pm/V, for the ZnSe cavity, and $n_{cl} = 2.38$ for the ZnSe/ZnS mirrors. For these parameters, the optimal core thickness is 0.3 μm ($m = 3$), which gives an effective index of $N_e = 2.40$ and an overlap integral $|J| = 0.0726 d_{eff}$. We assume that $L/w = 100$ and assume a vertical-cavity resonant enhancement of a factor of 400 in Eq. (1) to obtain $P_o/P_i^2 = 1\%/\text{W}$. Conversion efficiencies of the order of 10%/W could be obtained by incorporating a low-Q resonator for the fundamental or by vertical quasi-phase matching and perhaps 100%/W by combining these techniques. Comparable efficiencies are expected in the $Zn_xMg_{1-x}S_ySe_{1-y}$ material system,[9] in which a wide range of alloy compositions can be lattice matched to GaAs. Thus an optimized vertically resonant surface-emitting SHG device may be able efficiently to generate green or blue light in monolithic configurations with appropriate wide-band-gap semiconductors.

This work was supported by the Optoelectronics Materials Center and the Advanced Research Projects Agency through contract MDA972-90-C-0046.

References

1. R. Normandin and G. I. Stegeman, Opt. Lett. **4,** 58 (1979).
2. D. Vakhshoori, M. C. Wu, and S. Wang, Appl. Phys. Lett. **52,** 422 (1988).
3. A. Ashkin, G. D. Boyd, and J. M. Dziedzic, IEEE J. Quantum Electron. **QE-2,** 109 (1966).
4. R. Lodenkamper, M. M. Fejer, and J. S. Harris, Jr., Electron. Lett. **27,** 1882 (1991). We note a few typographical errors in this paper. Where ω appears as a factor in the definitions of the circulating power at the fundamental and second harmonic, and in Eqs. (8) and (11), it should be replaced by w, the width of the planar waveguide. In Eq. (6), α_0 should be α_ω. In Eq. (7), Λ should be L. Finally, in Eq. (12), U_x should be Ux.
5. R. Normandin, R. L. Williams, and F. Chatenoud, Electron. Lett. **26,** 2088 (1990).
6. K. Bacher, B. Pezeshki, S. M. Lord, and J. S. Harris, Jr., Appl. Phys. Lett. **61,** 1387 (1992).
7. H. A. MacLeod, *Thin Film Optical Filters,* 2nd ed. (Macmillan, New York, 1986), p. 519. For a resonator with the low-index layers of the mirrors adjacent to the cavity, the factor n_c/m in Eq. (5) should be replaced by $n_H n_L/m n_c$, where n_H and n_L are the indices of the high- and low-index mirror layers, respectively.
8. A. Arie, M. L. Bortz, M. M. Fejer, and R. L. Byer, Opt. Lett. **18,** 1757 (1993).
9. H. Okuyama, K. Nakano, T. Miyajima, and K. Akimoto, Jpn. J. Appl. Phys. **30,** L1620 (1991).